

Quantification of adipose tissue in a rodent model of obesity

David H. Johnson^a, Chris Flask^{a,b}, Dinah Wan^c, Paul Ernsberger^c, David L. Wilson^{a,b};
^aDept. of Biomedical Engineering, Case Western Reserve University, Cleveland, OH 44106;
^bDept. of Radiology, University Hospitals of Cleveland, Cleveland, OH 44106.
^cDept. of Nutrition, Case Western Reserve University, Cleveland, OH 44106.

ABSTRACT

Obesity is a global epidemic and a comorbidity for many diseases. We are using MRI to characterize obesity in rodents, especially with regard to visceral fat. Rats were scanned on a 1.5T clinical scanner, and a T1W, water-spoiled image (fat only) was divided by a matched T1W image (fat + water) to yield a ratio image related to the lipid content in each voxel. The ratio eliminated coil sensitivity inhomogeneity and gave flat values across a fat pad, except for outlier voxels (> 1.0) due to motion. Following sacrifice, fat pad volumes were dissected and measured by displacement in canola oil. In our study of 6 lean (SHR), 6 dietary obese (SHR-DO), and 9 genetically obese rats (SHROB), significant differences in visceral fat volume was observed with an average of 29 ± 16 ml increase due to diet and 84 ± 44 ml increase due to genetics relative to lean control with a volume of 11 ± 4 ml. Subcutaneous fat increased 14 ± 8 ml due to diet and 198 ± 105 ml due to genetics relative to the lean control with 7 ± 3 ml. Visceral fat strongly correlated between MRI and dissection ($R^2 = 0.94$), but MRI detected over five times the subcutaneous fat found with error-prone dissection. Using a semi-automated images segmentation method on the ratio images, intra-subject variation was very low. Fat pad composition as estimated from ratio images consistently differentiated the strains with SHROB having a greater lipid concentration in adipose tissues. Future work will include in vivo studies of diet versus genetics, identification of new phenotypes, and corrective measures for obesity; technical efforts will focus on correction for motion and automation in quantification.

Keywords: Obesity, MRI, small animal imaging, chemical selective imaging, body composition.

INTRODUCTION

Obesity is a global epidemic and a comorbidity for many diseases. We used the obese spontaneously hypertensive Koletsky rat (SHROB) to study obesity. This strain develops hypertension and obesity, and it does not express any isoforms of the leptin receptor.¹ We contrast the SHROB rat to the spontaneously hypertensive rat (SHR), which is genetically resistant to gaining weight, but it does gain weight on a special high fat, high sugar diet, which we call dietary obese (SHR-DO).² Comparisons of the genetically obese rats (SHROB) to dietary obese rats (SHR-DO) provide new insights into metabolic syndrome when compared against a control of SHR on a normal diet. Commonly summarized as metabolic syndrome, the overlapping conditions of hypertension, obesity, insulin resistance, and physical inactivity all increase risk of cardiovascular heart disease.³ SHROB rats provide a striking model for metabolic syndrome in humans because it develops all of these conditions.⁴ We investigate the effects of diet and genetics on visceral obesity, which is more clinically important than subcutaneous fat.⁵

Typical techniques for assessing obesity in rodents are limited in their accuracy (e.g. body mass index) or their invasiveness (e.g. dissection/lipid extraction). Hydrodensity (submersion) measurements require patient compliance not available with animal models,⁶ and electrical impedance measurements suffer from wide inaccuracy due to changes in animal hydration.^{7,8} In vivo imaging techniques include dual energy x-rays,^{9,10} CT,¹¹ and MRI.^{12,13} MRI can be used to measure fat pad volumes.¹⁴ It can also be used to measure percent lipid concentration per voxel using ratio images of fat/(fat+water)¹⁵. MR spectroscopy can be used for measurements of triglycerides, but the placement of the voxel makes a very large difference in the spectrum measured.¹⁶

We use MRI to assess visceral and subcutaneous fat for all three rodent groups identified above. We focus on MRI volume measurements of subcutaneous and visceral fat and compare results to dissection. We develop ratio imaging to provide an estimate of lipid content per voxel and to reduce coil sensitivity inhomogeneity. Lipid concentration is of great interest because it relates to triglyceride storage. We first describe the theory of ratio imaging. We then describe our imaging and analysis methods, followed by results and discussion.

THEORY

In the T1-weighted image sequence, the reconstructed T1-weighted magnitude image (ρ_1) where Λ contains various unknown constants including ADC gain, receive coil sensitivity, and factors depending on main field strength; ρ_0 is the spin density for fat and water indicated by respective subscripts; T1 relaxation is likewise defined (1). We neglect T2 relaxation effects due to the short TE used. We assume there is no change in the signal intensity due to changes in temperature because the imaging was done in approximately half an hour, and all animals survived.

$$\rho_1 = \Lambda \rho_{0,fat} \left(1 - e^{-\frac{T_R}{T_1,fat}}\right) + \Lambda \rho_{0,water} \left(1 - e^{-\frac{T_R}{T_1,water}}\right) \quad (1)$$

We assume perfect water suppression so there is no contribution from water. The reconstructed T1-weighted image acquired after the chemical shift selective pulse is ρ_2 (2).

$$\rho_2 = \Lambda \rho_{0,fat} \left(1 - e^{-\frac{T_R}{T_1,fat}}\right) \quad (2)$$

A parameter defined here as α can be used to capture and eliminate the effect of T1 weighting (4). This allows comparison of spin densities.

$$\alpha = \frac{1 - e^{-\frac{T_R}{T_1,fat}}}{1 - e^{-\frac{T_R}{T_1,water}}} \quad (3)$$

By assuming a value for both the T1 of fat and water which are not dependent on position we can simplify the model. In our imaging conditions at 1.5T and using long a TR, fat is far from its T1 and water is near to its T1. Therefore α is mostly determined by the T1 of water. Having captured the T1 effect, the water-suppression ratio image (R) is defined as the measurement of the number of fat spin density relative to the total spin density population in a given voxel (4).

$$R = \frac{\rho_{0,fat}}{\rho_{0,water} + \rho_{0,fat}} = \frac{\rho_2}{\rho_2 + \alpha(\rho_1 - \rho_2)} \quad (4)$$

Computing R requires knowledge of α , which can be evaluated from the definition (3). For the long TR used in these experiments (1240 ms), the effect of fat on α is minor because a typical fat T1 is 250 ms. Under our imaging conditions, the T1 of water will have contributions from both blood (T1 1200 ms) and from muscle (T1 900 ms). Considering these two cases, $\alpha = 1.3$ for blood and $\alpha = 1.5$ for muscle. The visceral and subcutaneous fat contains adipocytes and blood vessels, and as an approximation $\alpha = 1$ was used to process the images.

METHODS

1. Imaging

Seven SHROB, three SHR-DO, and six non-obese SHR were scanned in a Siemens Sonata 1.5T clinical scanner with two acquisitions done sequentially, each 15 min long. The rats were anesthetized by isoflurane and restrained within a phase-array coil on a tube which was designed to fit rats. The first MRI acquisition was a T1-weighted (T1W) spin echo acquisition (TR 1240 ms, TE 13 ms, resolution = 0.78x0.78x2mm, matrix = 256x128). The second scan was the same T1W acquisition preceded by a chemical shift selective (CHESS) water-suppression pulse (fat-only image).¹⁷

2. Image Analysis

The image sets were processed to segment the fat compartments using image processing techniques similar to those reported by other researchers.^{14,16,18} A study of inter-observer variability showed that measurements were not very dependent on the observer, so a single expert observer segmented all images. The boundary between subcutaneous and visceral fat was defined by manually tracing the peritoneum in each slice, and muscles and organs of the abdomen were removed by lower boundary thresholding at 0.5, corresponding to 50% lipid content. This threshold was very reproducible in the ratio images. Having defined subcutaneous fat was defined as fat not contained within the peritoneum, some additional manual corrections included removing bones and any other misclassified voxels as necessary. Total volume of the visceral and subcutaneous fat was computed from the number of voxels in each region multiplied by the volume of an individual voxel. Other researchers have reconstructed separate fat and water images from similar techniques, but their methods require making a T1 map of each subject.¹⁸

Further image processing was used to create a mask for eliminating errors in measuring voxel values in the water-suppression ratio images. The T1W, water-spoiled image was divided by the T1W image to yield an estimate of the ratio of the fat in each voxel as previously justified by the choice of $\alpha = 1$. For easier viewing, the air in the resulting image was set to zero. Air was determined by finding the mean and standard deviation of a 10x10 voxel region in each of the corners of the last slice of the T1-weighted image. Air was globally thresholded in each image volume at $\mu \pm 3\sigma$, where μ and σ are the mean and standard deviation respectively of the voxels in that region. Division by zero was eliminated by ignoring all voxels in the T1-weighted image with a value of 0. The effects of motion (peristalsis in the gastrointestinal tract, breathing, etc.) were reduced by excluding all voxels in the ratio image with values above 1. The partial volume effect was drastically reduced by calculating the magnitude of the 3D gradient and excluding the top 25% of voxels with the highest gradient magnitudes. Effectively, this step eliminated boundary voxels. All of these operations were combined to create a binary mask which was then multiplied with the water suppression ratio images.

The manual tracings of the peritoneum from the previous calculation of fat volume were loaded. The mean and standard deviation of the voxel values in the water suppression ratio images were calculated over the same voxels used to calculate the subcutaneous and visceral fat volumes with the exclusion of voxels outside the foreground mask.

3. Comparisons to dissection and statistical analyses of groups

The rats were sacrificed and dissected. The visceral fat pad was defined as the sum of mesenteric, gonadal, and retroperitoneal fat pads. Subcutaneous fat was dissected primarily from the subscapular fat pad. Fat pads were weighed, and volume was directly measured by displacement in canola oil.

An analysis of variance (ANOVA) tested for significant differences in voxel value due to the animal type (lean vs. dietary obese vs. genetically obese) and due to tissue type (subcutaneous vs. visceral fat). Separately, the volumes of subcutaneous and visceral fat pads were tested for significant differences due to the animal type, using R Project for Statistical Computing.¹⁹ Further statistical tests were done to correlate the volume of fat measured by MRI against the volume measured from dissection. P values below 0.05 were considered statistically significant.

RESULTS

Marked differences in size and fat distribution are apparent in typical MR images (Figure 1). The peritoneum is a dark ring in these coronal slices which has been manually traced to demarcate visceral fat. A set of SHROB images illustrate the creation of the ratio image (Figure 2, a-d). A sample water suppression ratio image without masking (Figure 3) shows the effects of peristalsis in the duodenum and misregistration due to motion near the heart; this justifies the exclusion of voxels above 1 in the water-suppression ratio image. The volume of each type of fat was compared to excised fat volumes from dissection both by weight (Figure 4). The effects of diet and genetics are apparent through the volumes of visceral and subcutaneous fat (Figure 5, a-b). These factors also influenced mean percent lipid stored in tissues, which was measured over the same voxels in the visceral and subcutaneous fat pads (Figure 6, a-b).

Statistics were computed to test for differences in percent lipid measurements. When voxel values were directly compared, the very high statistical power of the large number of voxels showed significant differences in all cases. Therefore the mean voxel values for visceral and subcutaneous fat were each reduced to their mean for each animal. The data for each animal was reduced to subcutaneous and visceral fat pad volumes and mean voxel in each of those fat

pads. An analysis of variance (ANOVA) test was used to show significant differences in mean voxel value due to the animal type (lean vs. dietary obese vs. genetically obese), which was significant in the water suppression ratio images ($P < 0.001$) but not in the T1-weighted images ($P = 0.29$).

Another ANOVA was used to show that visceral and subcutaneous adipose tissue depended on rat type. The genetically obese rats had significantly higher adipose tissue volumes than the lean controls. The genetic obese SHROB rats had significantly higher volumes of visceral and subcutaneous fat than the dietary obese SHR and the lean control SHR rats. The dietary obese SHR have a significantly higher volume of visceral fat than the lean control SHR rats.

DISCUSSION

In this animal model of Metabolic Syndrome X, these data suggest visceral fat results from both dietary and genetic obesity, but subcutaneous fat is unique to genetic obesity. We report the first measurements of percent lipid per voxel using this model of obesity. Fat pad composition as estimated from ratio images consistently differentiated the strains with SHROB having a greater lipid concentration in adipose tissues. These measurements provide new information about the in vivo composition of fat pads. As expected, the effects of diet and genetics both resulted in more volume of fat. Significant differences in visceral fat volume was observed with an average of 29 ± 16 ml increase due to diet and 84 ± 44 ml increase due to genetics relative to lean control with a volume of 11 ± 4 ml (Figure 5.a). Subcutaneous fat increased 14 ± 8 ml due to diet and 198 ± 105 ml due to genetics relative to the lean control with 7 ± 3 ml (Figure 5.b). These data can be used to phenotype rodents used in genetic exploration of obesity by characterizing fat volume, distribution, and composition.

Our analysis of lipid concentration per voxel is a good approximation. We chose MRI parameters such that $\alpha \approx 1$ in the fat pads. This reduces the calculation of fraction lipid to the simple ratio of the fat-only image divided by the T1W image. This approximation is appropriate for the long TR used in this experiment because the lipids have a short T1 and recover longitudinal magnetization quickly, making a larger (brighter) signal. Blood is the primary non-lipid signal in the fat pads. Blood has a much longer T1 than lipids; the slower recovery of these spins contrasts with the fat spins by a smaller (darker) signal. If measurement of fat within muscles is desired, $\alpha = 1.5$ would be a more accurate choice due to the differences in T1. The T1 of muscle (900 ms) is shorter than that of blood (1200 ms). Choosing α before running the sequence helps to pick a TR which maximizes the accuracy of the measurement of fraction of fat per voxel. The condition of α exactly equal to 1 corresponds to acquiring a proton density weighted image, but a true proton density is undesirable due the longer TR required, which contributes to significantly longer acquisition time (upwards of 45 minutes instead of 10 minutes). By making our approximations as justified here, the computation of R reduces to ρ_2 / ρ_1 with dependence on Λ eliminated (4). While this was convenient for this study, further acquisitions are needed to validate the conditions under which α can be approximated.

The ratio image eliminated coil sensitivity inhomogeneity, and this allowed us to develop a semi-automated segmentation method. A literature review revealed that ratio imaging makes the voxel values meaningful.¹⁵ The numerical value of each voxel represents the amount of fat (lipid) inside it in the logical range of 0 (no lipid) to 1 (pure lipid). Values above 1 were excluded because they are physically infeasible outliers. Inspection of the images indicates that the outlier values were probably due to motion, including peristalsis in the abdominal cavity, or due to ghosting from breathing artifacts or from image misregistration due to movement of the animal during the pair of long (10 min) acquisitions. Yet another possible explanation for values above 1 is that water suppression was not completely uniform due to main field strength variations, which is the main weakness of chemical shift selective pulses. One limitation of applying a chemical shift selective pulse to water is that its abundance in all tissues makes complete elimination of its signal unlikely, but under our imaging conditions it can be neglected relative to the noise inherent in acquisition of the MR signal.

The elimination of coil sensitivity inhomogeneity greatly aided the accuracy of manual segmentation. Visually, the ratio images are easier to read because the coil sensitivity inhomogeneity can obscure important edges, such as the outer boundary of the peritoneum. Intra-subject image segmentation variation was very low when using the water suppression ratio images and a fixed threshold corresponding to 50% lipid/voxel. This correction results in remarkably homogeneous regions of adipose tissue with reasonable percent lipid values. The remarkable homogeneity of gray value

in adipose tissue suggests automated segmentation algorithms currently under investigation. Researchers have reported success using an active contour to fit the peritoneum in T1W images.⁵

Visceral fat strongly correlated between MRI and dissection ($R^2 = 0.94$), but MRI detected over five times the subcutaneous fat found with error-prone dissection. There are intrinsic limitations of dissecting the subcutaneous and visceral fat pads. The subscapular fat pad was reliably excised and measured, but other subcutaneous fat pads often eluded dissection due to the challenge of reliably isolating them from surrounding tissues. Some researchers flay the animal and purify its skin in a blender to get an accurate measurement of subcutaneous fat.²⁰ The data suggest that volume and weight are linearly related and interchangeable by a density calculation (Figure 4), which lends support to using pure volume measurements such as MRI.

Future work will include correction for motion artifacts. The quantification of percent lipid of in vivo fat pads will yield new phenotypes for obesity. Future developments include using the more reliable voxel values to write an automatic segmentation algorithm, which will enable large scale studies of body composition in obese rodents.

ACKNOWLEDGEMENTS

We would like to thank the Ernsberger/Koletsky lab and the Small Animal Imaging Resource Center. This work was supported by Ohio Wright Center of Innovation and Biomedical Research and Technology Transfer award: "The Biomedical Structure, Functional and Molecular Imaging Enterprise." This investigation was conducted in a facility constructed with support from Research Facilities Improvement Program Grant Number C06 RR12463-01 from the National Center for Research Resources, National Institutes of Health.

REFERENCES

- 1 S Koletsky, "New type of spontaneously hypertensive rats with hyperlipemia and endocrine gland defects," *Spontaneous Hypertension: Its Pathogenesis and Complications*, vol. pp. 194-197, (1972).
- 2 S.Rattigan, P.R.Howe, and M.G.Clark, "The effect of a high-fat diet and sucrose drinking option on the development of obesity in spontaneously hypertensive rats," *British Journal of Nutrition*, vol. 56, pp. 73(1986).
- 3 S.M.Grundy, "Small LDL, atherogenic dyslipidemia, and the metabolic syndrome," *Circulation*, vol. 95, pp. 1-4, (1997).
- 4 D.P.Wan, D.H.Johnson, J.L.Johnson, R.J.Koletsky, C.Flask, and P.Ernsberger, "Magnetic Resonance Imaging of Visceral and Subcutaneous Fat Distribution in Genetic Versus Dietary Obesity," *Obesity Research*, vol. 13, pp. A172(2005).
- 5 G.Iacobellis, "Imaging of visceral adipose tissue: an emerging diagnostic tool and therapeutic target," *Current drug targets - Cardiovascular & haematological disorders*, vol. 5, pp. 345-353, (2005).
- 6 R.Johnson, "Fitting percentage of body fat to simple body measurements," *Journal of Statistics Education*, vol. 4, (1996).
- 7 B.L.Heitmann, "Prediction of body water and fat in adult Danes from measurement of electrical impedance. A validation study," *International Journal of Obesity*, vol. 14, pp. 789-802, (1990).
- 8 K.R.Segal, B.Gutin, E.Presta, J.Wang, and T.B.Van Itallie, "Estimation of human body composition by electrical impedance methods: a comparative study," *Journal of applied physiology (Bethesda, Md.: 1985)*, vol. 58, pp. 1565-1571, (1985).
- 9 M.D.Jensen, J.A.Kanaley, J.E.Reed, and P.F.Sheedy, "Measurement of abdominal and visceral fat with computed tomography and dual-energy x-ray absorptiometry," *American Journal of Clinical Nutrition*, vol. 61, pp. 274-278, (1995).
- 10 E.G.Kamel, G.McNeill, and M.C.Van Wijk, "Usefulness of anthropometry and DXA in predicting intra-abdominal fat in obese men and women," *OBESITY RESEARCH*, vol. 8, pp. 36-42, (2000).
- 11 K.van der Kooy and J.C.Seidell, "Techniques for the measurement of visceral fat: a practical guide," *International Journal of Obesity*, vol. 17, pp. 187-196, (1993).
- 12 W.Shen, Z.Wang, M.Punyanita, J.Lei, A.Sinav, J.G.Kral, C.Imielinska, R.Ross, and S.B.Heymsfield, "Adipose tissue quantification by imaging methods: a proposed classification," *OBESITY RESEARCH*, vol. 11, pp. 5-16, (2003).

- 13 D.D.Brennan, P.F.Whelan, K.Robinson, O.Ghita, J.M.O'Brien, R.Sadleir, and S.J.Eustace, "Rapid automated measurement of body fat distribution from whole-body MRI," *American Journal of Roentgenology*, vol. 185, pp. 418-423, (2005).
- 14 S.R.Smith and J.J.Zachwieja, "Visceral adipose tissue: a critical review of intervention strategies," *International Journal of Obesity*, vol. 23, pp. 329-335, (1999).
- 15 E.Lunati, P.Marzola, E.Nicolato, and A.Sbarbati, "In-vivo quantitative hydrolipidic map of perirenal adipose tissue by chemical shift imaging at 4.7 Tesla," *International Journal of Obesity*, vol. 25, pp. 457-461, (2001).
- 16 L.Wilhelm Poll, H.J.Wittsack, J.A.Koch, R.Willers, M.Cohnen, C.Kapitza, L.Heinemann, and U.Modder, "A rapid and reliable semiautomated method for measurement of total abdominal fat volumes using magnetic resonance imaging," *Magnetic resonance imaging*, vol. 21, pp. 631-636, (2003).
- 17 A.Haase, J.Frahm, W.Hanicke, and D.Matthaei, "1H NMR chemical shift selective (CHESS) imaging," *Physics in Medicine and Biology*, vol. 30, pp. 341-344, (Apr 1, 1985).
- 18 E.Lunati, P.Marzola, E.Nicolato, M.Fedrigo, M.Villa, and A.Sbarbati, "In vivo quantitative lipidic map of brown adipose tissue by chemical shift imaging at 4.7 Tesla," *Journal of Lipid Research*, vol. 40, pp. 1395-1400, (1999).
- 19 R Development Core Team. *R: A language and environment for statistical computing*, (R Foundation for Statistical Computing, Vienna, Austria,2005).
- 20 H.Tang, J.R.Vasselli, E.X.Wu, C.N.Boozer, and D.Gallagher, "High-resolution magnetic resonance imaging tracks changes in organ and tissue mass in obese and aging rats," *American journal of physiology.Regulatory, integrative and comparative physiology.*, vol. 282, pp. R890-R899(2002).

FIGURES

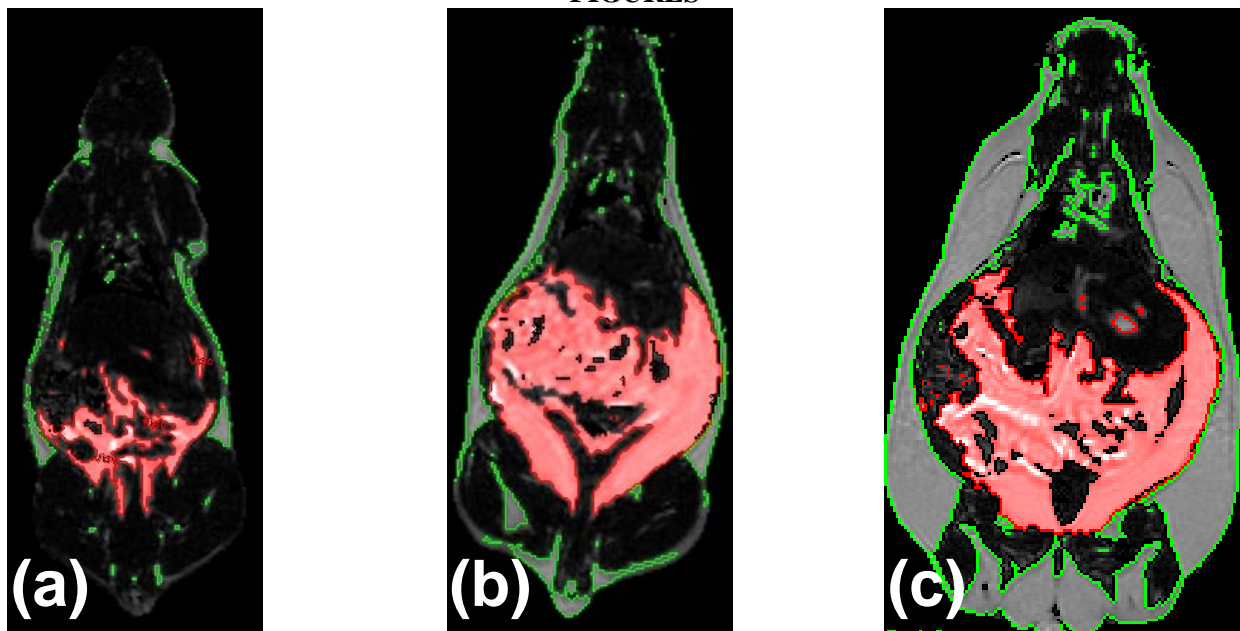
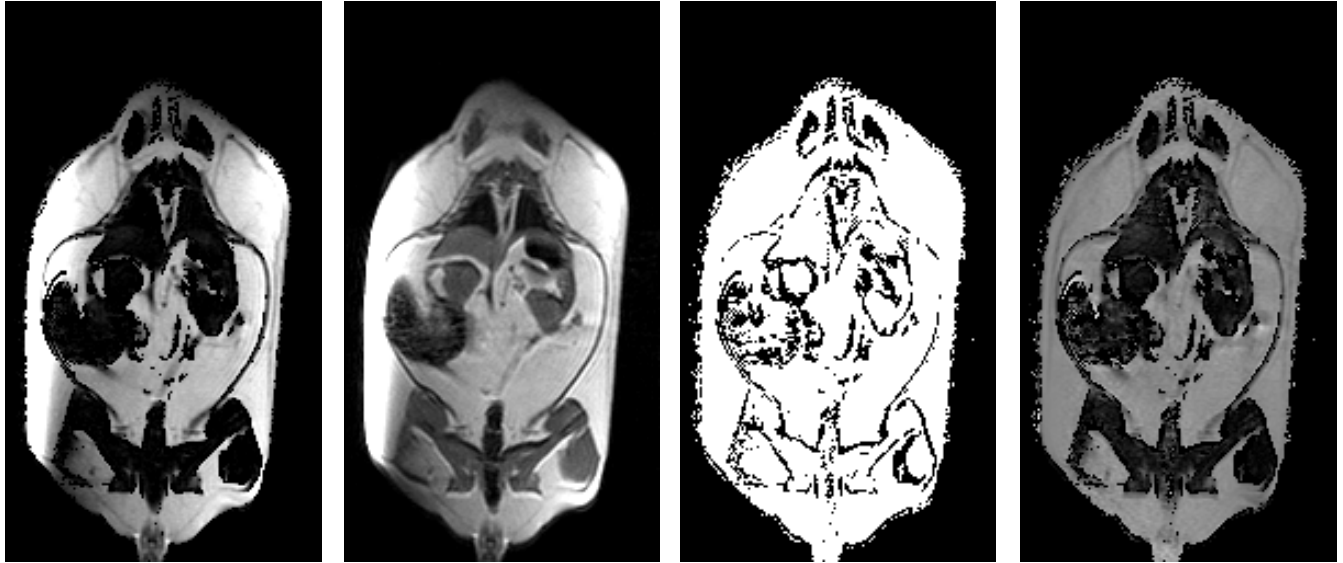


Figure 1. Comparison of typical MR images of the different strains: lean control SHR (a), dietary obese SHR-DO (b), and genetically obese (c). The visceral and subcutaneous fat is traced in red and green, respectively. Some intramuscular fat is mislabeled as subcutaneous in (b); this is manually corrected along with the removal of bones.



(a) Fat-only image (b) T1-weighted (T1W) image (c) Mask (no air, etc) (d) Water suppression ratio image

Figure 2. Ratio imaging of a genetically obese rat (SHROB). Note the variability of brightness on the left side of the T1-weighted fat-only image (a) caused by coil sensitivity inhomogeneity, which is also present in the T1-weighted image (b). After removing the voxels outside the mask (c), coil sensitivity inhomogeneity is eliminated in the ratio image (d).

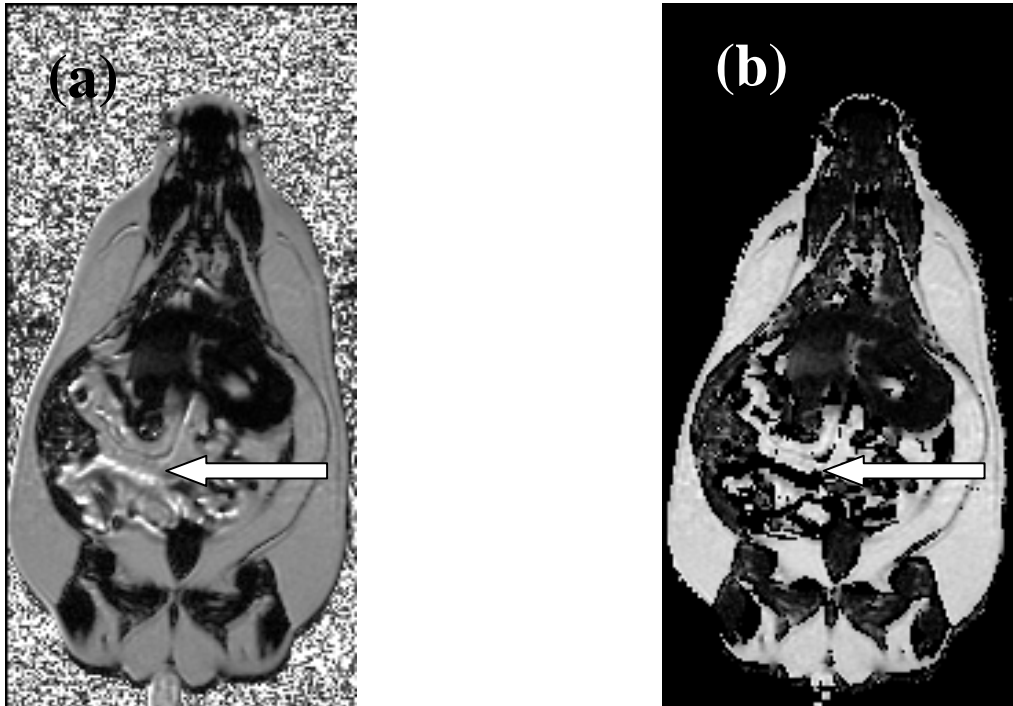


Figure 3. An uncorrected ratio image (a) shows motion artifacts in the in the digestive tract indicated by the arrow. The corrected ratio image (b) shows that such physically meaningless, high voxel values (> 1.0) have been removed.

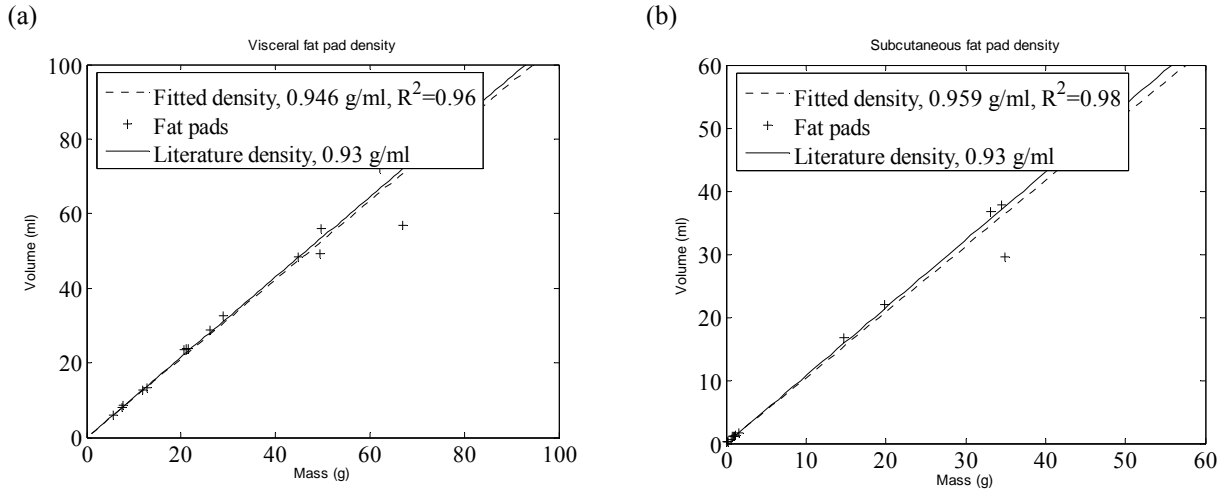


Figure 4. Comparison of dissection weight to volume. The excised fat pads were weighed, and their volumes were measured by displacement in canola oil. The close fit to the literature density (solid line) indicates that there was little muscle or other tissues contaminating the dissection.

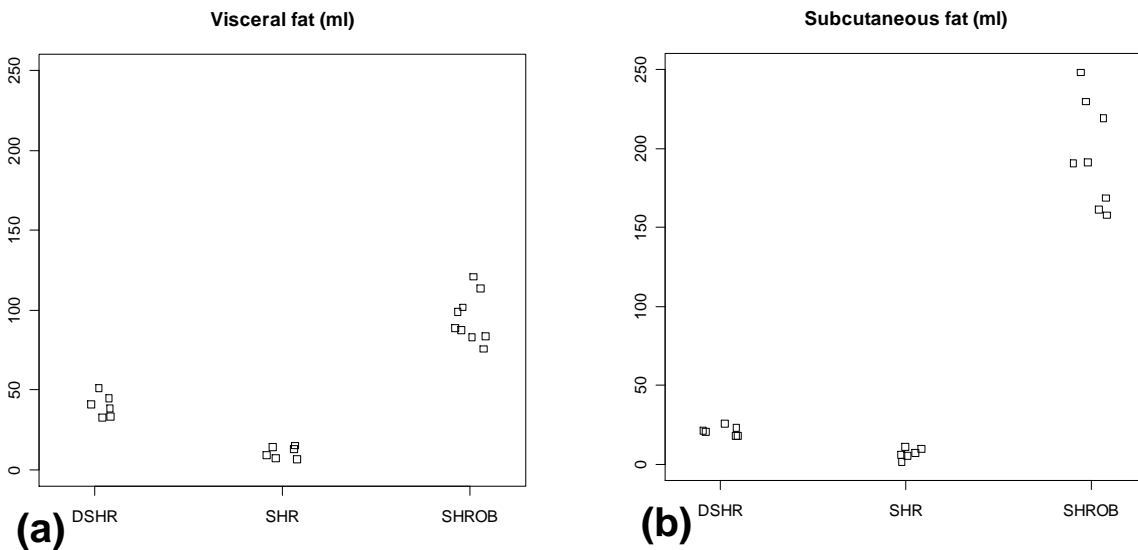


Figure 5. Volumes measured by MRI. The genetic obese SHROB rats have significantly higher volumes of visceral and subcutaneous fat than the dietary obese SHR and the lean control SHR rats. The dietary obese SHR have a significantly higher volume of visceral fat than the lean control.

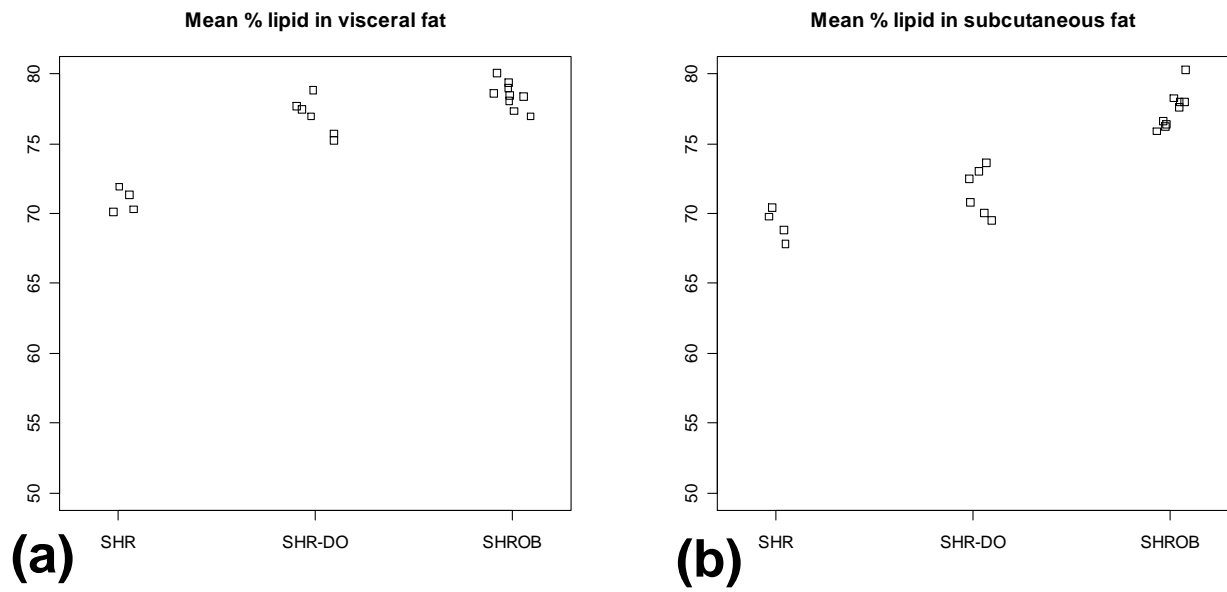


Figure 6. Mean percent lipid in the visceral (a) and subcutaneous (b) fat depots as a function of diet and genetics. These values reflect an estimate of triglyceride storage. In visceral fat both diet and genetics increase storage of triglycerides. Genetics but not diet appears to increase the mean % lipid in subcutaneous fat.